Rock and Soil Mechanics

Volume 44 | Issue 12 Article 2

2-7-2024

Energy evolution of unloading confining pressure and dissipative energy damage constitutive model of coal-rock combination

Wen-kai RU
School of Energy and Mining Engineering, Shandong University of Science and Technology, Qingdao, Shandong 266590, China; School of Resources and Safety Engineering, Central South University, Changsha, Hunan 410083, China, ruwenkai@csu.edu.cn

Shan-chao HU
School of Energy and Mining Engineering, Shandong University of Science and Technology, Qingdao, Shandong 266590, China, mining2@126.com

Di-yuan LI
School of Resources and Safety Engineering, Central South University, Changsha, Hunan 410083, China

Jin-yin MA
School of Resources and Safety Engineering, Central South University, Changsha, Hunan 410083, China

See next page for additional authors

Recommended Citation

RU, Wen-kai; HU, Shan-chao; LI, Di-yuan; MA, Jin-yin; ZHANG, Chen-xi; LUO, Ping-kuang; GONG, Hao; and ZHOU, Ao-hui (2024) "Energy evolution of unloading confining pressure and dissipative energy damage constitutive model of coal-rock combination," *Rock and Soil Mechanics*: Vol. 44: Iss. 12, Article 2.
DOI: 10.16285/j.rsm.2022.6883
Available at: https://rocksoilmech.researchcommons.org/journal/vol44/iss12/2

Energy evolution of unloading confining pressure and dissipative energy damage constitutive model of coal-rock combination

Abstract

In coal mining, the excavation of a coal-rock roadway and a thin coal seam will inevitably cause radial unloading of the coal-rock combination system. The radial unloading phenomenon is often accompanied by the rapid accumulation and release of energy, so it is necessary to investigate the energy evolution law of coal-rock combination specimens under the unloading confining pressure condition. To this end, the unloading confining pressure tests with different unloading rates were carried out for the coal-rock combination specimens. The results show that: (1) The axial loading and constant stress stages are the main energy storage stages of the combination specimens. The failure stage is mainly dominated by the release and dissipation of energy. (2) The acceleration of the unloading rate leads to the decrease of the peak elastic energy of the specimens, and the increment of the elastic energy at 0.03 MPa /s in the constant stress stage is 1.64, 2.70 and 3.50 times of that at 0.06 MPa /s, 0.09 MPa /s, and 0.12 MPa /s, respectively. (3) The increase of unloading rate will lead to the increase of post-peak dissipation energy of the specimen, and the post-peak dissipation energy is 28.17%, 49.53%, 69.55% and 92.87% of the peak elastic energy when the unloading rate increases from 0.03 MPa /s to 0.12 MPa /s, respectively. (4) The increase in unloading rate will significantly enhance the tensile failure tendency of coal-rock combination specimens, resulting in an increase in the fracture angle, an increase in the number of tensile secondary cracks, and an enhancement in the breaking strength. (5) A dissipative energy constitutive model considering the initial damage is established to reasonably explain the whole process of damage evolution of coal-rock combination specimens under the unloading confining pressure conditions. The research results are significant for understanding the energy evolution characteristics of coal-rock combination samples with unloading rate.

Keywords

coal-rock combination, unloading confining pressure, energy, damage, constitutive equation

Authors

Wen-kai RU, Shan-chao HU, Di-yuan LI, Jin-yin MA, Chen-xi ZHANG, Ping-kuang LUO, Hao GONG, and Ao-hui ZHOU

Rock and Soil Mechanics 2023 44(12): 3448−3458 ISSN 1000−7598
https: //doi.org/10.16285/j.rsm.2022.6883 https://rocksoilmech.researchcommons.org/journal/

Energy evolution of unloading confining pressure and dissipative energy damage constitutive model of coal-rock combination

RU Wen-kai[1, 2], HU Shan-chao[1], LI Di-yuan[2], MA Jin-yin[2], ZHANG Chen-xi[2], LUO Ping-kuang[2], GONG Hao[2], ZHOU Ao-hui[2]

1. School of Energy and Mining Engineering, Shandong University of Science and Technology, Qingdao, Shandong 266590, China
2. School of Resources and Safety Engineering, Central South University, Changsha, Hunan 410083, China

Abstract: In coal mining, the excavation of a coal-rock roadway and a thin coal seam will inevitably cause radial unloading of the coal-rock combination system. The radial unloading phenomenon is often accompanied by the rapid accumulation and release of energy, so it is necessary to investigate the energy evolution law of coal-rock combination specimens under the unloading confining pressure condition. To this end, the unloading confining pressure tests with different unloading rates were carried out for the coal-rock combination specimens. The results show that: (1) The axial loading and constant stress stages are the main energy storage stages of the combination specimens. The failure stage is mainly dominated by the release and dissipation of energy. (2) The acceleration of the unloading rate leads to the decrease of the peak elastic energy of the specimens, and the increment of the elastic energy at 0.03 MPa /s in the constant stress stage is 1.64, 2.70 and 3.50 times of that at 0.06 MPa /s, 0.09 MPa /s, and 0.12 MPa /s, respectively. (3) The increase of unloading rate will lead to the increase of post-peak dissipation energy of the specimen, and the post-peak dissipation energy is 28.17%, 49.53%, 69.55% and 92.87% of the peak elastic energy when the unloading rate increases from 0.03 MPa /s to 0.12 MPa /s, respectively. (4) The increase in unloading rate will significantly enhance the tensile failure tendency of coal-rock combination specimens, resulting in an increase in the fracture angle, an increase in the number of tensile secondary cracks, and an enhancement in the breaking strength. (5) A dissipative energy constitutive model considering the initial damage is established to reasonably explain the whole process of damage evolution of coal-rock combination specimens under the unloading confining pressure conditions. The research results are significant for understanding the energy evolution characteristics of coal-rock combination samples with unloading rate.

Keywords: coal-rock combination; unloading confining pressure; energy; damage; constitutive equation

1 Introduction

The depth of mining in China is increasing year by year due to the imminent exhaustion of shallow coal resources[1]. Complex conditions in deep strata often induce geotechnical engineering disasters such as roadway deformation and instability, roof fall and rock burst. The occurrence of these geologic hazards is not determined solely by coal or rock strata in most instances, but largely affected by the integrated structure of coal-rock combination system[2−5], which is worthy of systematic study. In the process of mining and excavation, the life cycle of rockmass from stabilization to destruction is often accompanied by the input, accumulation, dissipation and release of energy. Therefore, it is more valuable to investigate the deformation and failure of coal-rock combination structure from the perspective of energy.

Restricted by the research conditions at the engineering site, scholars have carried out a lot of indoor tests on the energy evolution of coal-rock combination structures. Zuo et al.[6] determined the energy evolution law of coal-rock combination specimens under the axial loading condition through uniaxial tests, and constructed a model of differential energy instability based on energy analysis. Chen et al.[7−8] and Yang et al.[9] conducted uniaxial tests on coal-rock combination specimens with different height ratios and determined their pre-peak energy evolution law. Zuo et al.[10] and Yang et al.[11] conducted uniaxial compression tests under cyclic loading and unloading on coal, rock, and coal-rock combination specimens, to comparatively obtain the energy evolution law and to reveal the damage mechanisms. In addition, many scholars[12−14] have investigated the nonlinear evolution characteristics of coal-rock combination under axial cyclic loading and unloading. Through comparison, it can be found that at present, the acquisition of the energy evolution law and energy criterion of coal-rock combination, and the construction of damage evolution constitutive model are mostly carried out through the data obtained from uniaxial loading, conventional triaxial loading as well as axial loading and unloading tests, the unloading of the combination specimens, however, has rarely been involved in the confining pressure unloading

Received: 2 December 2022 Accepted: 28 March 2023
This work was supported by the National Natural Science Foundation of China (5190040670, 52274087) and the Natural Science Foundation of Shandong Province (ZR2023ME189).
First author: RU Wen-kai, male, born in 1995, PhD candidate, focusing on deep resource mining and rock mechanics. E-mail: ruwenkai@csu.edu.cn
Corresponding author: HU Shan-chao, male, born in 1984, PhD, Associate Professor, research interests: rock mechanics. E-mail: mining2@126.com

tests. It should be pointed out that in coal mine production, the radial unloading of coal-rock combination structure caused by roadway excavation and working face mining is always the root cause of some geologic disasters. Therefore, it is necessary to study the energy evolution law of coal-rock combination under confining pressure unloading conditions, to reveal the damage mechanism of coal-rock combination structure, and to construct the damage constitutive model applicable to coal-rock combination under confining pressure unloading conditions.

Although few studies have been conducted on the confining pressure unloading characteristics of coal-rock combination, the energy evolution of pure rock/pure coal specimens under confining pressure unloading conditions has been well addressed. Dai et al.[15] summarized the pre-peak unloading energy evolution law of pure rock specimens under different stress paths. Zhu et al.[16] and Xu et al.[17] disclosed the energy dissipation characteristics of pure rock specimens under unloading conditions by carrying out unloading tests on pure rock specimens under different confining pressures. Cong et al.[18] and Li et al.[19] obtained the energy evolution characteristics of marble under different confining pressure unloading paths by carrying out confining pressure unloading tests. Based on the above research on the energy evolution of pure rock specimens, many scholars have paid attention to the constitutive model of pure rock specimens. Ma et al.[20] derived the relationship between unloading rate and energy of pure rock specimens by carrying out triaxial unloading tests under different unloading rates, and also analyzed their damage characteristics, thereby proposing a constitutive model considering energy damage. On this basis, some scholars have summarized the unloading constitutive models of rock, describing the current progress of research on the constitutive models of rock under confining pressure unloading conditions[21−22]. It should be noted that the above results embarked on the energy characteristics of pure rock unloading from various aspects so as to construct constitutive models applicable to the unloading characteristics, but they have not taken into account the existence of initial damage in the rockmass with primary defects, and the constructed damage variables and constitutive equations can hardly describe the coal with obvious initial compaction stage. It is thereby necessary to consider the initial damage to establish a constitutive model suitable for confining pressure unloading of coal-rock combination specimens.

In summary, this paper takes coal-rock combination as the research object, carries out confining pressure unloading tests with different unloading rates, discusses the energy evolution law at different stages, and obtains the relationship between unloading rate and energy evolution. From the perspective of dissipated energy evolution and confining pressure damage characteristics, this study proposes a dissipated energy damage variable considering the native defects inside the specimen, and construct a dissipated energy damage constitutive model applicable to the confining pressure unloading damage. The research results are of great significance for understanding the energy evolution characteristics of coal-rock combination specimens under different confining pressure unloading rates.

2 Specimen preparation and test schemes

2.1 Specimen preparation

The coal and rock samples used in this study were taken from the Qiwu Coal Mine of Shandong Energy Zaozhuang Mining Group in China, which is a typical rock burst mine. The main coal seam in the No. 4 Mining Area currently being mined is the Lower 3# Coal Seam, whose seam structure is complex. The thickness of the Lower 3# Coal is 1.08−4.78 m, with an average of 3.34 m. The height of the semi coal-rock roadway is 4.00 m. The roof of the roadway mainly consists of 7.8−20.2 m thick fine sandstone that possesses a strong bursting liability.

Coal and rock specimens were cored by drilling from the 3# Coal Seam and the roof strata. The collected coal and rock specimens were prepared into cylinders with a diameter×height of 50 mm×50 mm and polished at both ends. After preparation, in order to mimic the cementation characteristics between coal and rock strata in the engineering site, coal and rock specimens were bonded with AB glue[23−24] in accordance with the size ratio of 1:1, and made into 50 mm×100 mm coal-rock combination specimens. Finally, all the standard specimens were placed at room temperature for 24 hours to solidify the colloid. The specimens after the completion of preparation are shown in Fig. 1. In order to simplify the test and dig into the effect of unloading rate on the energy evolution of coal-rock combination, only the specimens with a coal-rock height ratio of 1:1 was selected for study, and the coal-rock height ratio and inclination angle were all kept fixed.

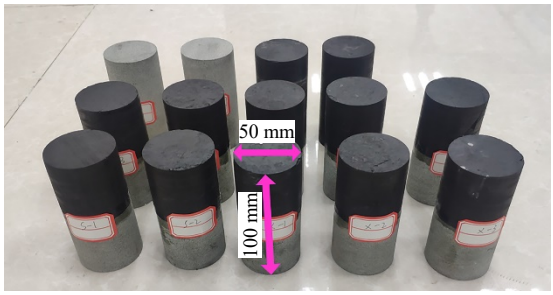

Fig. 1 Part of coal-rock combination samples

2.2 Test scheme

The conventional triaxial loading and unloading confining pressure tests were performed on the RLJW-2000 microcomputer-controlled rock servo three-axis, shear (creep) testing machine in Shandong University of Science and Technology. The test principle is shown in Fig. 2. The testing machine is loaded from the bottom upward so as to more closely match the in-site coal and rock combination structure that acts as the main bearing area. The bottom plane of the rock is taken as the bearing surface, and the rock from the coal-rock combination is placed underneath while the coal is placed on the top, as shown in Fig. 2.

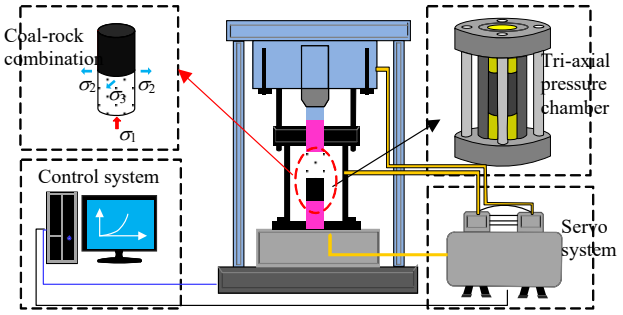

Fig. 2 Test device and principle

During the test, the tests under the same conditions were conducted three times and the average test result was selected and analyzed as follows:

Scenario I: Conventional triaxial loading test

In order to obtain the conventional triaxial loading strength, deformation parameters and damage characteristics to provide a reference for the unloading test, the stress-controlled loading method was adopted with a loading rate of 0.05 MPa /s. According to the results of in-situ stress measurements from a mine shaft, the maximum horizontal principal stress of the 3# Coal Seam is 11.4−13.3 MPa, so the confining pressure of the conventional triaxial loading test is set to be 10 MPa, and the corresponding peak strength σ_c is 71.69 MPa.

Scenario II: Triaxial confining pressure unloading test

Based on the conventional triaxial loading test, the triaxial confining pressure unloading test was conducted following the procedure shown in Table 1. The test is divided into three steps: (i) the confining pressure σ_3 is loaded to 10 MPa at a rate of 0.05 MPa /s; (ii) the axial pressure σ_1 is loaded to 70% of the peak strength of the conventional triaxial loading test (50.18 MPa) at a rate of 0.05 MPa /s[25−26], and σ_1 is maintained at a constant level; and (iii) the confining pressure is unloaded at the rates of 0.03, 0.06, 0.09 MPa /s, and 0.12 MPa /s respectively to the point that the specimen is completely broken, and the indicator of complete damage is that the stress−strain curve slowly decreases or basically remains constant after the peak. The loading and unloading paths and parameter settings for the conventional triaxial loading test and triaxial unloading test are shown in Fig. 3. Throughout the test, the axial strain of the combination specimen was measured by an axial extensometer. A circumferential extensometer was placed on the coal side where the main dilatation occurred.

Table 1 Unloading rates of confining pressures and initial stress conditions

Test scheme	Initial confining pressure /MPa	Initial axial stress /MPa	Confining pressure unloading rate /(MPa • s^{-1})
Scenario I: Conventional triaxial loading test	10	10	—
Scenario II: Triaxial confining pressure unloading test	10	0.7σ_c	0.03
			0.06
			0.09
			0.12

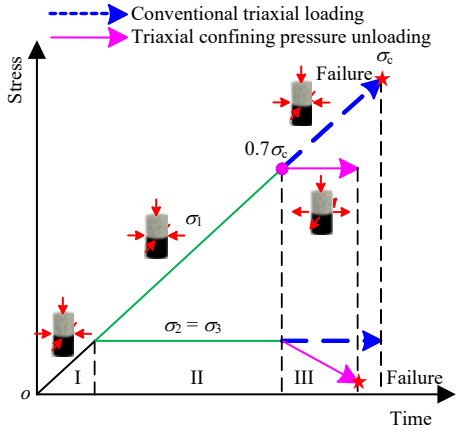

Fig. 3 Loading and unloading paths for conventional triaxial loading and triaxial unloading confining pressure tests

3 Different stress paths

3.1 Principle of energy calculation

In the conventional triaxial loading test, the total energy U of the specimen can be expressed as

$$U = U_1 + U_3 = U_e + U_d \tag{1}$$

where U_1, U_3, U_e and U_d are the energy input from the work done by axial stress, the energy input from the work done by confining pressure, the accumulated elastic energy and the dissipated energy, respectively, each of which can be expressed explicitly as[16−17]

$$\left.\begin{aligned} U_1 &= \sum_{i=1}^{n}\frac{1}{2}\left(\sigma_1^i+\sigma_1^{i+1}\right)\left(\varepsilon_1^{i+1}-\varepsilon_1^i\right)\\ U_3 &= \sum_{i=1}^{n}\left(\sigma_3^i+\sigma_3^{i+1}\right)\left(\varepsilon_3^{i+1}-\varepsilon_3^i\right)\\ U_e &= \frac{1}{2E}\left[\sigma_1^2+2\sigma_3^2-2\nu\sigma_3\left(2\sigma_1+\sigma_3\right)\right]\\ U_d &= U-U_e \end{aligned}\right\} \tag{2}$$

where n is the number of segments of the stress−strain curve; i is the segment point; σ_1 is the axial stress; σ_3 is the confining pressure; ε_1 is the axial strain; and ε_3 is the circumferential strain; and $\overline{E}$ and $\overline{v}$ are the elasticity modulus and Poisson's ratio in the linear elastic stage, respectively.

In the triaxial confining pressure unloading test, axial load exerts compressive stress on the specimen end, and the change of confining pressure rate only affects the circumferential stress level of the specimen. If the stress state at each moment is analyzed separately, it can be found that each moment of the triaxial confining pressure unloading test is equivalent to an individual conventional triaxial loading test. Therefore, the energy calculation Eq. (1) and Eq. (2) under conventional triaxial loading conditions are suitable for energy calculation in confining pressure unloading test[20].

3.2 Conventional triaxial loading test

According to the design of the test scheme, the energy evolution of the conventional triaxial loading test is presented in Fig. 4.

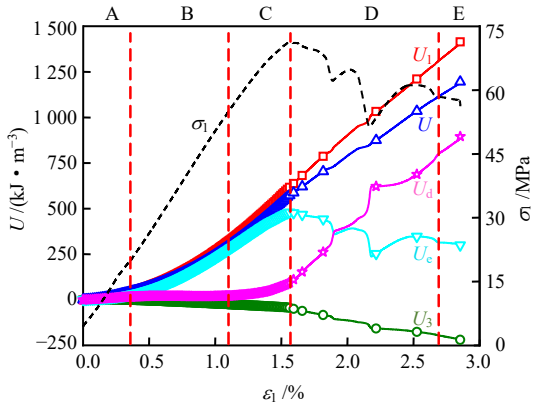

Fig. 4 Energy evolution curves of conventional triaxial loading test

In the compaction stage (A), the axial input energy U_1, elastic energy U_e and total energy U all increase with the increase of axial strain, and the differences among them are very small. At the same time, the confining pressure input energy U_3 shows an obvious downward trend, while the dissipated energy U_d gradually declines, indicating that there is energy dissipation when the internal cracks of the specimen are closed in the compaction stage. It is therefore necessary to study the initial damage characteristics of the specimen at the compaction stage.

In the linear elasticity stage (B), U_e, U and U_1 experience similar trends, showing concave-up increase with increasing growth rate of axial strain. U_d remains basically unchanged, indicating a small quantity of newly formed cracks in the specimen with increasing axial stress, and naturally, the loss of energy accounts for a very small part. At the same time, there is a significant negative growth in U_3, indicating that the circumferential strain of coal-rock combination increases considerably from this stage.

Plastic yielding stage (C): as the axial stress continues to increase, the stress−strain curve presents a nonlinear growth, the microcracks inside the specimen gradually increase, the circumferential deformation and volumetric deformation gradually increase, and the coal begins to show obvious circumferential dilatation, with ever-increasing growth in U_d and U_3. The axial stress is always at a high stress level and the rate of increase of U_1 remains essentially unchanged, still increasing at a fast rate, but the growth rates of U_e and U fall off slightly.

Instability and failure stage (D): the internal microcracks are connected, forming a macroscopic fracture on the specimen surface. Elastic energy U_e is released rapidly and converted into energy dissipated by the failure of the specimen. Meanwhile, circumferential deformation increases sharply, which is manifested as rapid growths of U_d and U_3, thus further slowing down the increase of U. There is still no significant change in the growth rate of U_1.

Residual strength stage (E): The axial stress slowly decreases, and the coal-rock combination enters the residual strength stage, where U_1 still increases at a higher rate whereas U slowly increases. U_d and U_3 go up continuously while U_e continues to come down, all at a significantly lower rate.

3.3 Triaxial confining pressure unloading test

In this study, a total of four groups of confining pressure unloading tests were carried out, in which the energy evolution curves of coal-rock combination specimens at the unloading rate of 0.03 MPa /s are shown in Fig. 5.

Among them, the energy characteristics of the compaction stage (a), linear elasticity stage (b) and residual strength stage (e) are basically similar to those of the conventional triaxial loading curves, and thus only the energy characteristics of the constant axial stress stage (c) and instability and failure stage (d) are analyzed in this section.

Constant axial stress-confining pressure unloading stage (c): after the onset of unloading, axial stress remains stable and the growth rate of U_1 keeps steady; the growth rate of circumferential strain is further accelerated compared with that in the linear elasticity stage, and the negative growth of U_3 is enhanced little by little, which results in that U does not show a significant increase. In addition, U_d plummets in this stage, against the steady and minor build-up of U_e. This is because although the deepened damage degree of coal enlarges the amplitude of dissipated

energy, the entire specimen still holds a high capacity for energy accumulation, and thus the elastic energy gradually increases. Since the dissipated energy is the difference between the total energy and elastic energy, the total energy remains essentially stable so that the dissipated energy appears to decline.

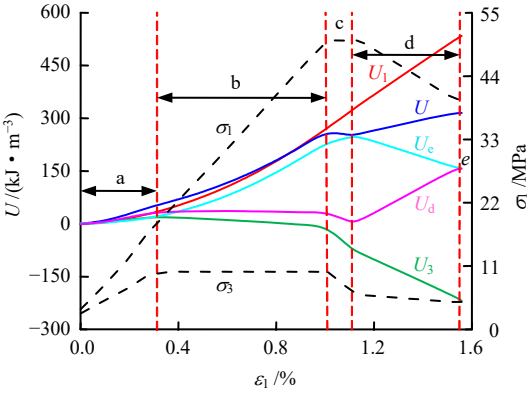

(a) Energy−axial strain curve

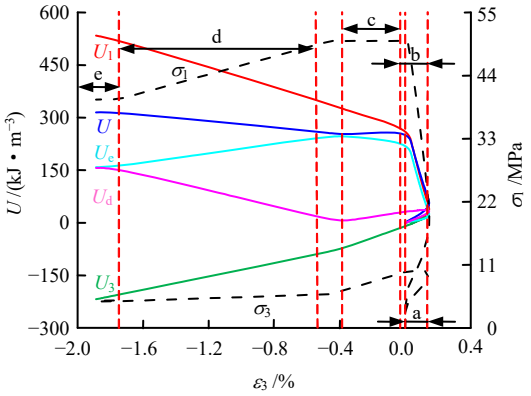

(b) Energy−circumferential strain curve

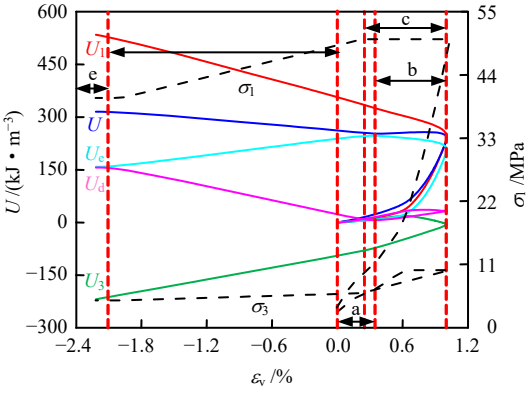

(c) Energy−volumetric strain curve

Fig. 5 Evolution curve of energy in triaxial confining pressure unloading test(confining pressure is 10 MPa, unloading rate of confining pressure is 0.03 MPa /s)

Instability and failure stage (d): The combination specimen reaches the energy storage limit at the end of stage c, so U_e hits the peak. Along with the continuous unloading, principal stress difference is further intensified, microcracks inside the coal develop extensively and then connect with each other to form macrocracks. The specimen is gradually destabilized with U_d rising drastically. In the meantime, due to the broken of coal, the energy accumulation ability of the combination specimen falls, resulting in a rapid energy release, a plunge of U_e and a zoom-up of U_3. Although the axial bearing capacity of the specimen gradually decreases, the increase of axial strain has no obvious effect on the growth rate of U_1, and the total energy U increases at a small rate. Compared with the constant axial stress stage at which the energy is mainly accumulated, energy dissipation is dominated at this stage.

According to the energy−circumferential strain curve in Fig. 5(b) and the energy−volumetric strain curve in Fig. 5(c), it is found that the relationship between energy and circumferential/volumetric strain during the loading stage is the same as that of the axial strain. After the commence of unloading, circumferential strain and volumetric strain increase in the reverse direction, and a clear dilatation is gradually emerging. While U_1 continues to climb, U_d increases positively and U_3 increases negatively. Since U_d and U_3 reflect the internal damage degree and volumetric deformation of the specimen respectively, it can be seen that there is a certain correlation between the damage and volumetric expansion of the specimen during the test.

Comparing the energy evolution characteristics of the combination specimens under two stress paths, it is found that the specimen is dominated by energy storage before the peak of conventional triaxial loading, and by energy release and dissipation after the peak; energy storage prevails in the loading stage of confining pressure unloading test and constant axial stress stage, whereas the energy release and dissipation take the lead in the stage of instability and failure. Mutual conversion of energy triggers the development, extension and coalescence of cracks within the specimen, resulting in the deepening of damage degree and ultimate instability and failure.

4 Different confining pressure unloading rates

4.1 Relationship between energy evolution characteristics and unloading rate

The variations of elastic energy and dissipated energy with axial strain for coal-rock combination specimens under different confining pressure unloading rates are given in Figs. 6 and 7.

(1) The relationship between the elastic energy and confining pressure unloading rate is depicted in Fig. 6. The loading and unloading stages of the confining pressure−strain curve of the specimen under the unloading rate of 0.03 MPa /s are divided. There is no significant difference in the elastic energy of each specimen in the axial loading stage, and the strain energy curves in the early loading

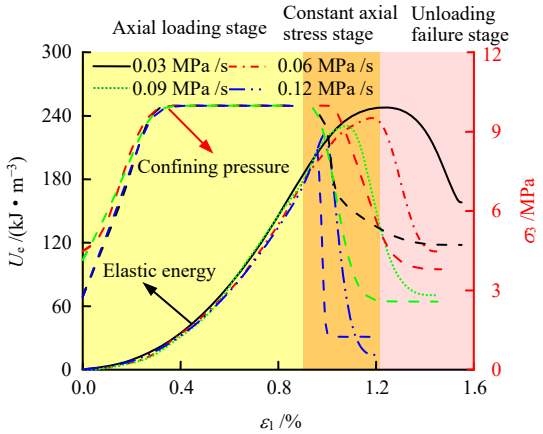

Fig. 6 Comparison curve of strain energy

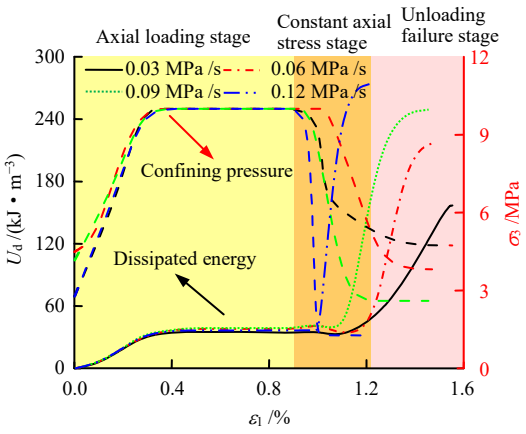

Fig. 7 Comparison curve of dissipated energy

stage are concave up due to the compaction and closure of primary microcracks. After the cracks are completely closed, the curve begins to rise linearly up to 70% of the peak strength, entering the linear elastic stage. Keeping the axial load constant, microcracks inside the coal develop rapidly after the onset of unloading, but the elastic energy curve presents a convex growth. After the specimen begins to fracture, the elastic energy curve drops abruptly, followed by a stable period. This indicates that the energy storage capacity of the combination specimen undergoes a process of firstly increasing[18, 20], then rapidly decreasing and finally stabilizing. Comparing the elastic energy curve under each unloading rate, it can be found that in the confining pressure unloading stage, the larger the unloading rate is, the less elastic energy is left after the failure of the specimen.

(2) Figure 7 shows the relationship between the dissipated energy and confining pressure unloading rate. The loading and unloading stages of the confining pressure−strain curve of the specimen under the unloading rate of 0.03 MPa /s are divided. Similar to the elastic energy, the dissipated energy curve of each specimen in the loading stage are close to each other, with the difference that they begin to stabilize after an upward concave growth, further indicating that the specimen is in the linear elastic stage at this moment. After entering the confining pressure unloading stage, the dissipated energy curve shows an obvious S-shaped growth, first stabilizing, then rising rapidly, and finally turning downward. It means that the energy released by the combination specimen in this loading-unloading stage has gone through the process of basically not releasing at first, then releasing rapidly, and finally changing to no longer releasing again. Comparing the dissipated energy curve under each unloading rate, it can be found that during the unloading stage, the faster the unloading rate is, the faster the rate of energy release is, resulting in the eventual dissipation of more energy.

4.2 Relationship between peak elastic energy and unloading rate

The values of each energy index for the coal-rock specimens at the peak stress under different unloading rates are listed in Table 2.

Table 2 Energy values of stress peaks at different unloading rates of confining pressure

Unloading rate /(MPa • s^{-1})	Post-peak failure time /s	Peak energy /(kJ • m^{-3})				
		U_1	U_3	U_e	U_d	U
0.03	755	422.2	−106.4	255.6	60.2	315.8
0.06	420	385.9	−88.2	243.2	54.5	297.7
0.09	290	344.1	−64.7	232.3	47.1	279.4
0.12	180	284.6	−21.8	224.7	38.0	262.7

Table 2 suggests that the energy values of coal-rock combination specimens at the stress peak are gradually reduced with the increase of unloading rate, which is because the larger the unloading rate, the faster the reduction rate of confining pressure, resulting in the specimen being destabilized more quickly, and the time for continuous energy accumulation being shortened. As the unloading rate increases, the time required for post-peak failure is shortened, resulting in less elastic energy accumulated at the stress peak.

4.3 Characteristics of energy conversion in constant axial stress stage

In order to accurately evaluate the energy characteristics of coal-rock combination specimen in constant axial stress stage, the incremental difference ΔU($\Delta U = U_f - U_j$) was obtained by subtracting the elastic energy U_j at the end of the loading stage from the elastic energy U_f at the stress peak, as shown in Fig. 8.

The variation of each energy value in the constant axial stress stage decreases with increasing confining pressure unloading rate, but is affected by the unloading rate to different extent. Numerically, the energy changes ΔU_1, ΔU_3, ΔU_e, ΔU_d and ΔU of the combination specimen

at the unloading rate of 0.03 MPa /s are 1.34, 1.23, 1.54, 1.64, and 1.41 times that of the unloading rate of 0.06 MPa /s, 2.22, 1.80, 3.46, 2.70, and 5.70 times that of the unloading rate of 0.09 MPa /s, and 8.96, 15.58, 5.42, 3.50, 23.03 times that at 0.12 MPa /s, respectively, as shown in Table 3. The above statistics reveal that the sensitivities of different types of energy are different against the confining pressure unloading rate. Among them, the most significant effect is on ΔU_d, indicating that the unloading rate has a greater influence on the initiation and expansion of cracks inside the coal-rock specimen.

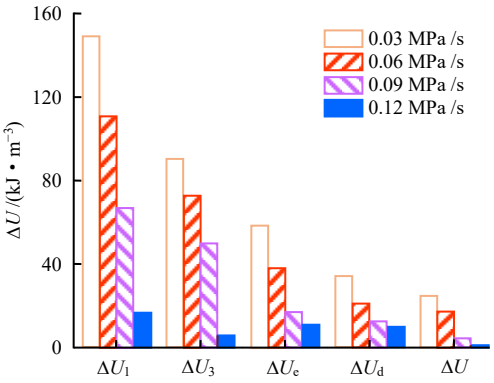

Fig. 8 Energy characteristic of the axial stress constant stage under different unloading rates

4.4 Energy changes in axial loading and unloading stages

Figure 9 compares the variation of each energy value of the coal-rock specimen in the loading stage and unloading stage (constant axial stress stage and unloading failure stage) under different unloading rates.

In Fig. 9, the axial loading stage is the main energy accumulation stage for the specimen, and the variations of energy in the loading stage are approximately the same. From the beginning of the constant axial stress stage to the end of the unloading failure stage, there is an obvious difference in the amount of change in each energy. With the increase of unloading rate, the changes in U_1 and U_3 decrease while the changes in U_e and U_d increase gradually. The reason is that the increase of U_1 is always kept at a high level, and the faster the unloading rate is, the faster the specimen breaks, and the less the $\Delta U_{1unload}$ is. For U_3, according to Eq. (2), the level of circumferential stress is the main controlling factor in determining the change of U_3, and the faster the unloading rate is, the smaller the circumferential stress is at the time of failure, and the less $\Delta U_{3unload}$ it is. When the confining pressure unloading rate is 0.03, 0.06, 0.09 and 0.12 MPa /s respectively, $\Delta U_{eunload}$ is 28.17%, 49.53%, 69.55% and 92.87% of the elastic energy accumulated in the corresponding axial loading stage. The reason is that a faster unloading of confining pressure releases more energy in a short time. The corresponding $\Delta U_{dunload}$ is 3.37, 4.51, 4.68 and 6.16 times of the dissipated energy accumulated in the axial loading stage, which gradually increases with increasing unloading rate. It further indicates a faster energy release and a more sudden failure of the specimen subjected to a higher unloading rate.

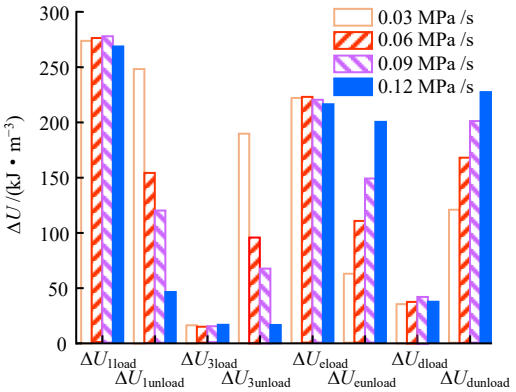

Fig. 9 Energy comparison in loading and unloading stages at different unloading confining pressure rates

4.5 Failure strength

According to the study of Chen et al.[27], under the same initial confining pressure, the faster the unloading rate, the smaller the maximum strain energy that can be stored before failure, the more elastic energy released after peak, and the higher the failure strength after instability. To this end, the energy characteristics of coal-rock specimens were determined statistically by the changes in loading energy and unloading energy under different confining pressure unloading rates, as shown in Table 3. From the table, the faster the unloading rate, the smaller the energy change in the loading stage, decreasing gradually from 255.6 kJ /m^3 at 0.03 MPa /s to 224.7 kJ /m^3. Energy variation in unloading stage increases bit by bit with the increase of unloading rate, ranging from 62.4 kJ /m^3 to 199.7 kJ /m^3, indicating that the failure strength of the coal-rock combination specimen gradually increases with the acceleration of unloading rate, which is the same as that of pure rock sample.

Table 3 Changes of loading energy and unloading energy under different confining pressures

Unloading rate /(MPa • s^{-1})	Loading energy change /(kJ • m^{-3})	Unloading energy change /(kJ • m^{-3})
0.03	255.6	62.4
0.06	243.2	110.1
0.09	232.3	148.4
0.12	224.7	199.7

4.6 Failure mode

The failure modes of combination specimens under

different confining pressure unloading rates are displayed in Fig. 10. The yellow lines mark the macrocracks and the white lines are secondary cracks. In general, the cracks in the combination specimens appear on only the side of coal, and there is a main shear crack cutting through the coal, showing obvious single shear failure. The confining pressure unloading rate increases from 0.03 MPa /s to 0.12 MPa /s, and the fracture angle, correspondingly, increases from 62.2º to 74.4º. A large number of secondary cracks are distributed near the shear main crack. With the increase of unloading rate, secondary cracks in the vicinity of the shear main crack increase inch by inch, occurring in the direction approximately perpendicular to the unloading direction. Generally, with the increase of unloading rate, the confining effect on the specimen is weakened rapidly, accompanied with an increased likelihood of tensile failure.

In addition, with the increase of unloading confining pressure rate, conspicuous sloughing appears at the top and lower right of the coal, which is due to the excessive energy released per unit time due to an accelerated expansion of cracks. This phenomenon further verifies the proportional relationship between the unloading rate and failure strength discussed in section 4.5.

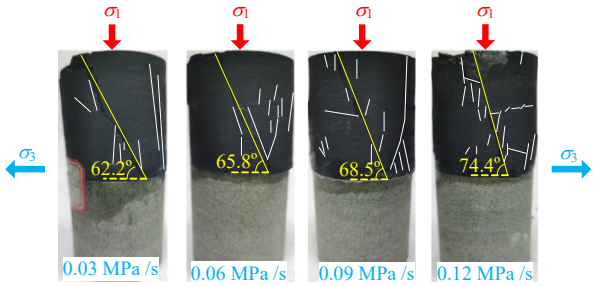

Fig. 10 Failure modes of coal-rock combination samples at different unloading rates

5 Damage constitutive model

5.1 Damage evolution equation

Based on previous studies[29−31], Liu et al.[28] analyzed the damage variable obtained from the number of acoustic emission events of pure coal specimens under uniaxial loading, and redefined the damage variable as

$$D_{\mathrm{L}}=\left(1-\frac{\sigma_{1\mathrm{s}}}{\sigma_{1\mathrm{c}}}\right)\frac{C_{\mathrm{d}}}{C_0} \tag{3}$$

The damage constitutive model is

$$\sigma=\left(1-D_{\mathrm{L}}\right)E\varepsilon=\left[1-\left(1-\frac{\sigma_{1\mathrm{s}}}{\sigma_{1\mathrm{c}}}\right)\frac{C_{\mathrm{d}}}{C_0}\right]E\varepsilon \tag{4}$$

where D_{L} is the damage variable; $\sigma_{1\mathrm{s}}$ is the residual strength; $\sigma_{1\mathrm{c}}$ is the peak axial stress; C_{d} is the cumulative number of acoustic emission events when the damage region of the material reaches A_{d}; C_0 is the cumulative acoustic emission event count.

Ma et al.[20] also reconstructed the damage variable from the energy point of view based on Eq. (5):

$$D_{\mathrm{M}}=\left(1-\frac{\sigma_{1\mathrm{s}}}{\sigma_{1\mathrm{c}}}\right)\frac{U_{\mathrm{d}}}{U_{\mathrm{dmax}}} \tag{5}$$

The damage constitutive model is

$$\sigma_1=2\mu\sigma_3+\left[1-\left(1-\frac{\sigma_{1\mathrm{s}}}{\sigma_{1\mathrm{c}}}\right)\frac{U_{\mathrm{d}}}{U_{\mathrm{dmax}}}\right]E\varepsilon_1 \tag{6}$$

where D_{M} is the damage variable; U_{d} is the dissipated energy when the damage region of the cross-section reaches A_{d}; and U_{dmax} is the cumulative dissipated energy required for complete failure.

The coal in the combination specimens usually contains abundant initial defects, so the coal-rock specimens undergo an obvious compaction process at the beginning of loading, i.e., the compaction stage described above, and the stress−strain curves and the energy curves both exhibit obvious downward concave segments. For this reason, this paper proposes the energy index U_{d0}, the energy used to close the initial damage, to quantify the closure degree of primary cracks at the early loading stage, based on the characteristic that the initial damage closure consumes energy.

In addition, the axial stress during unloading first remains constant and then gradually decreases, but the damage has begun to accumulate at an accelerated rate, which is somewhat different from the change of axial stress. Compared to the axial stress, confining pressure starts to decrease from the beginning of unloading, which is more in line with the accumulation of damage. Therefore, σ_{s} is considered to be converted into the confining pressure at the time of complete failure $\sigma_{3\mathrm{s}}$, and σ_{c} is assumed to be converted into the initial confining pressure $\sigma_{3\mathrm{c}}$.

Based on Eq. (7), the characterization method of damage variable considering initial damage is proposed:

$$D=\left(1-\frac{\sigma_{3\mathrm{s}}}{\sigma_{3\mathrm{c}}}\right)\frac{\left|U_{\mathrm{d}}-U_{\mathrm{d0}}\right|}{U_{\mathrm{dmax}}} \tag{7}$$

where U_{d0} is the energy dissipated by initial damage, which takes the value of the dissipated energy at the end of the compaction stage (the total dissipated energy when the dissipated energy curve remains constant and the elastic energy curve grows linearly), and D is the damage variable. Due to the existence of numerous primary defects in coal, the closure of primary cracks in the loading process will dissipate a certain amount of energy. Therefore, U_{d0} is taken as the energy to be dissipated for primary cracks closure, and its value is greater than 0, indicating that

the specimen has suffered damage before loading. In order to accurately characterize the damage degree of the combination specimen, the absolute value of U_d−U_{d0} is taken to characterize the damage variable D.

According to the research results of elastic mechanics, the stress−strain constitutive relationship of rocks considering damage characteristics can be expressed as

$$\sigma_1 = 2\bar{\mu}\sigma_3 + \bar{E}(1-D)\varepsilon_1 \tag{8}$$

Substituting Eq. (7) into Eq. (8) yields the dissipated energy damage constitutive equation considering the initial damage

$$\sigma_1 = 2\bar{\mu}\sigma_3 + \left[1-\left(1-\frac{\sigma_{3s}}{\sigma_{3c}}\right)\frac{|U_d - U_{d0}|}{U_{dmax}}\right]\bar{E}\varepsilon_1 \tag{9}$$

5.2 Validation of damage constitutive equation

According to the damage variable expression (7) and dissipated energy damage constitutive equation (9), the damage variable and axial stress of coal-rock combination specimens under different unloading rates are fitted, and the relationship between the experimental results and fitting curves are compared in Fig. 11, where the scattered dots are experimental results, the solid line is the evolution of damage variable based on Eq. (7), the dotted line is the stress−strain curve based on Eq. (9), and the dash line is the stress−strain curve based on Eq. (10).

$$\sigma_1 = 2\bar{\mu}\sigma_3 + \left[1-\left(1-\frac{\sigma_{1s}}{\sigma_{1c}}\right)\frac{|U_d - U_{d0}|}{U_{dmax}}\right]\bar{E}\varepsilon_1 \tag{10}$$

Figure 11 also plots the evolution curves of damage variable during loading and unloading stages at different unloading rates. The damage variable of each specimen before loading is kept around 11%, which corresponds to the presence of a host of primary cracks in coal. After the axial stress is applied, the damage variable gradually decreases until it vanishes after the primary cracks are completely closed. Axial stress continuing to be applied, the damage variable remains at zero, which is similar to the characteristics of the damage variable evolution obtained from pure coal specimens in conventional triaxial loading tests in previous studies[32−33]. The development rate of microcracks inside the specimen accelerates after the beginning of unloading. The damage variable increases exponentially, and stabilizes again after the specimen is completely damaged. The evolution of the damage variable matches the energy characteristics of the coal-rock specimen at different stages during the above unloading process. Moreover, the faster the unloading rate is, the larger the damage variable is after failure, which also matches the relationship between dissipated energy and unloading rate discussed above.

Comparing the stress−strain curves fitted according to Eq. (9) and Eq. (10) in Fig. 11, it is found that the

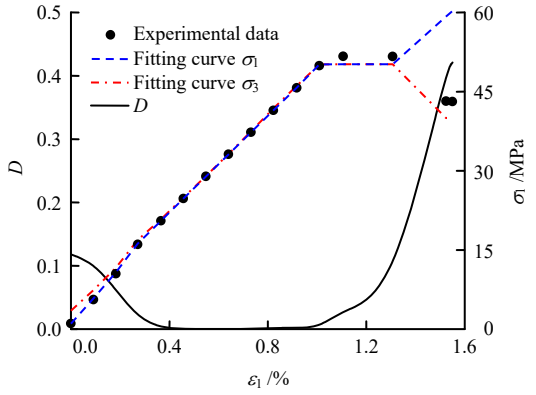

(a) 0.03 MPa /s

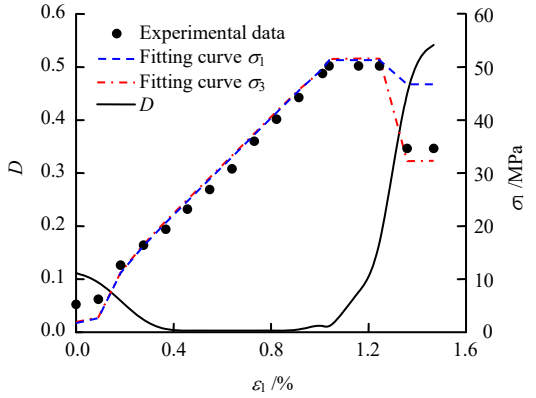

(b) 0.06 MPa /s

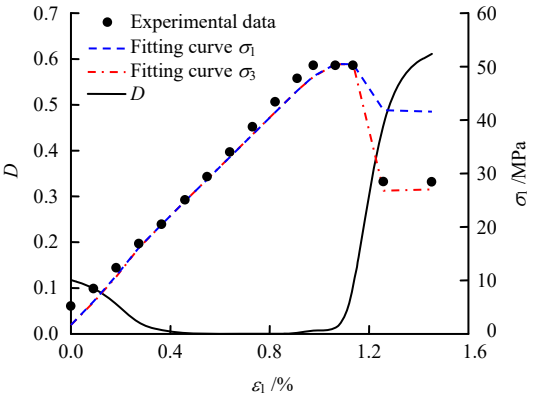

(c) 0.09 MPa /s

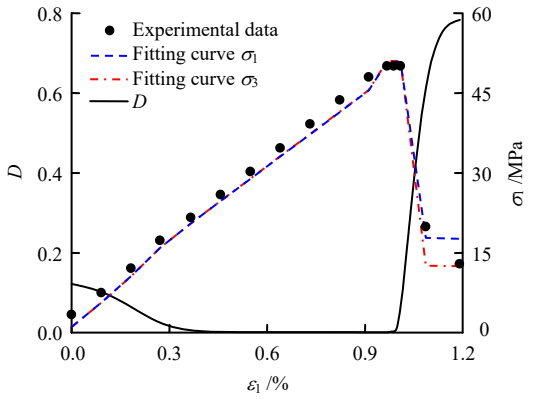

(d) 0.12 MPa /s

Fig. 11 Test results and fitting curves of coal-rock combination samples under confining pressure unloading

curves fitted with axial and circumferential stress intensity can precisely highlight the stress characteristics of the combination specimen before instability. However, in the simulation of the post-peak curve, the fitting degree between the curve obtained by fitting the intensity of the circumferential stress and the experimental data is significantly higher than that of the axial stress. It indicates that under the confining pressure unloading condition, the change of confining pressure is more sensitive to specimen's damage degree, and the constitutive model constructed on the basis of circumferential stress is therefore more applicable. The dissipated energy damage variable and damage constitutive equation are able to accurately describe the damage evolution of coal-rock specimen in different unloading and failure processes.

6 Conclusions

In this paper, the energy evolution characteristics of coal-rock combination specimens under different confining pressure unloading rates are investigated, and the relationship between failure strength and unloading rate is evaluated. The following conclusions can be drawn:

(1) Under the triaxial confining pressure unloading path, the loading stage and the constant axial stress stage are the main energy storage stages, while the instability and failure stage is mainly dominated by energy release and dissipation.

(2) All energy values at the stress peak decrease gradually with the increase of unloading rate. The faster the unloading rate, the less elastic energy and dissipated energy at the stress peak, and the less residual elastic energy and the more dissipated energy after complete failure.

(3) The increase of unloading rate will increase the fracture angle of the coal-rock combination specimens. When the confining pressure unloading rate increases from 0.03 MPa /s to 0.12 MPa /s, the fracture angle, as a consequence, increases from 62.2º to 74.4º. The increase of unloading rate also leads to an increase in the number of secondary cracks. An obvious sloughing is encountered at the unloading rate of 0.12 MPa /s, indicating that the failure strength is substantially enhanced with the increase of unloading rate.

(4) Based on the dissipated energy and circumferential stress characteristics, a dissipated energy damage variable and a damage constitutive model considering the initial damage are established. The constructed damage variable can effectively capture the initial damage and other stages of the damage of the combination specimen. The constitutive model constructed based on the circumferential stress shows advantages over the constitutive model based on the axial stress in fitting the indoor test results, especially in the residual strength stage.

References

[1] HE Man-chao, XIE He-ping, PENG Su-ping, et al. Study on rock mechanics in deep mining engineering[J]. Chinese Journal of Rock Mechanics and Engineering, 2005, 24(16): 2803−2813.

[2] LIU Jian-xin, TANG Chun-an, ZHU Wan-cheng, et al. Rock-coal model for studying the rockburst[J]. Chinese Journal of Geotechnical Engineering, 2004, 26(2): 276−280.

[3] LIU Cong-liang, TAN Zhi-xiang, DENG Ka-zhong, et al. Synergistic instability of coal pillar and roof system and filling method based on plate model[J]. International Journal of Mining Science and Technology, 2013, 23(1): 145−149.

[4] ZHU Zhuo-hui, FENG Tao, GONG Feng-qiang, et al. Experimental research of mechanical properties on grading cycle loading-unloading behavior of coal-rock combination bodies at different stress levels[J]. Journal of Central South University (Science and Technology), 2016, 47(7): 2469−2475.

[5] ZUO Jian-ping, CHEN Yan, WANG Chao. Failure mechanics and models for deep coal-rock combination[M]. Beijing: Science Press, 2017: 1−11.

[6] ZUO Jian-ping, SONG Hong-qiang. Energy evolution law and differential energy instability model of coal-rock combined body[J]. Journal of China Coal Society, 2022, 47(8): 3037−3051.

[7] CHEN Guang-bo, LI Tan, ZHANG Guo-hua, et al. Experimental study on the law of energy accumulation before failure of coal-rock combined body[J]. Journal of China Coal Society, 2021, 46(Suppl. 1): 174−186.

[8] CHEN Guang-bo, ZHANG Jun-wen, HE Yong-liang, et al. Derivation of pre-peak energy distribution formula and energy accumulation tests of coal-rock combined body[J]. Rock and Soil Mechanics, 202, 43(Suppl. 2): 130−143, 154.

[9] YANG Lei, GAO Fu-qiang, WANG Xiao-qing. Mechanical response and energy partition evolution of coal-rock combinations with different strength ratios[J]. Chinese Journal of Rock Mechanics and Engineering, 2020, 39(Suppl.2): 3297−3305.

[10] ZUO Jian-ping, XIE He-ping, MENG Bing-bing, et al. Experimental study on loading-unloading behavior of coal-rock combination bodies at different stress levels[J]. Rock and Soil Mechanics, 2011, 32(5): 1287−1296.

[11] YANG Lei, GAO Fu-qiang, WANG Xiao-qing, et al. Energy evolution law and failure mechanism of coal-rock combined specimen[J]. Journal of China Coal Society, 2019, 44(12):

3894−3902.

[12] CHEN Yan, ZUO Jian-ping, WEI Xu, et al. Energy nonlinear evolution characteristics of failure behavior of coal-rock combined body[J]. Journal of Underground Space and Engineering, 2017, 13(1): 124−132.

[13] MOU Zong-long, WANG Hao, PENG Peng, et al. Experimental study on failure characteristics and bursting liability of rock-coal-rock sample[J]. Journal of Mining and Safety Engineering, 2013, 30(6): 841−847.

[14] CHEN Yan, ZUO Jian-ping, SONG Hong-qiang, et al. Deformation and crack evolution of coal-rock combined body under cyclic loading-unloading effects[J]. Journal of Mining and Safety Engineering, 2018, 35(4): 826−833.

[15] DAI Bing, ZHAO Guo-yan, YANG Chen, et al. Energy evolution law of rocks in process of unloading failure under different paths[J]. Journal of Mining and Safety Engineering, 2016, 33(2): 367−374.

[16] ZHU Ze-qi, SHENG Qian, XIAO Pei-wei, et al. Analysis of energy dissipation in process of unloading confining pressure failure of rock[J]. Chinese Journal of Rock Mechanics and Engineering, 2011, 30(Suppl.1): 2675−2681.

[17] XU Guo-an, NIU Shuang-jian, JING Hong-wen, et al. Experimental study of energy features of sandstone under loading and unloading[J]. Rock and Soil Mechanics, 2011, 32(12): 3611−3617.

[18] CONG Yu, WANG Zai-quan, ZHENG Ying-ren, et al. Energy evolution principle of fracture propagation of marble with different unloading stress paths[J]. Journal of Central South University (Science and Technology), 2016, 47(9): 3140−3147.

[19] LI Di-yuan, SUN Zhi, LI Xi-bing, et al. Mechanical response and failure characteristics of granite under different stress paths in triaxial loading and unloading conditions[J]. Chinese Journal of Rock Mechanics and Engineering, 2016, 35(Suppl.2): 3449−3457.

[20] MA De-peng, ZHOU Yan, LIU Chuan-xiao, et al. Energy evolution characteristics of coal failure in triaxial tests under different unloading confining pressure rates[J]. Rock and Soil Mechanics, 2019, 40(7): 2645−2652.

[21] LI Jian-he, SHENG Qian, ZHU Ze-qi, et al. Research progress of mechanical characteristics and constitutive model of rock under unloading condition[J]. Journal of Yangtze River Scientific Research Institute, 2017, 34(7): 87−93.

[22] HUANG Da, TAN Qing, HUANG Run-qiu. Mechanism of strain energy conversion process for marble damage and fracture under high stress and rapid unloading[J]. Chinese Journal of Rock Mechanics and Engineering, 2012, 31(12): 2483−2493.

[23] DU Xue-ling. Discussion on national standard of burst tendency of combined coal and rock[J]. Coal Mine Safety, 2020, 51(10): 229−235, 242.

[24] YU Wei-jian, WU Gen-shui, LIU Ze, et al. Uniaxial compression test of coal-rock-bolt anchorage body and mechanical mechanisms of bolts[J]. Chinese Journal of Rock Mechanics and Engineering, 2020, 39(1): 57−68.

[25] WANG Le-hua, NIU Cao-yuan, ZHANG Bing-yi, et al. Experimental study on mechanical properties of deep-buried soft rock under different stress paths[J]. Chinese Journal of Rock Mechanics and Engineering, 2019, 38(5): 973−981.

[26] LU Xi-gen, JI Hong-guang, YU Xiao-mei, et al. Mechanical characteristics and energy dissipation evolution of coal under triaxial unloading[J]. Journal of Harbin Institute of Technology, 2022, 54(2): 90−98.

[27] CHEN Wei-zhong, LÜ Sen-peng, GUO Xiao-hong, et al. Research on unloading confining pressure tests and rockburst criterion based on energy theory[J]. Chinese Journal of Rock Mechanics and Engineering, 2009, 28(8): 1530−1540.

[28] LIU Bao-xian, HUANG Jing-lin, WANG Ze-yun, et al. Study on damage evolution and acoustic emission character of coal-rock under uniaxial compression[J]. Chinese Journal of Rock Mechanics and Engineering, 2009, 28(Suppl.1): 3234−3238.

[29] BARILE C, CASAVPLA C, PAPPALETTERA G, et al. Damage characterization in composite materials using acoustic emission signal-based and parameter-based data[J]. Composites Part B-Engineering, 2019, 178: 107469.

[30] MAO Da-wei, DU Shao-hua, LI Di-yuan, et al. Mechanical behaviors and wetting-induced deformation of metamorphic granite based on large-scale triaxial test[J]. Chinese Journal of Rock Mechanics and Engineering, 2020, 39(9): 1819−1831.

[31] SEVOSIANOV I, VERIJENKO V, KACHANOV M. Cross-property correlations for short fiber reinforced composites with damage and their experimental verification[J]. Composites Part B-Engineering, 2002, 33(3): 205−213.

[32] YANG Sheng-qi, XU Peng, RANJITH P G. Damage model of coal under creep and triaxial compression[J]. International Journal of Rock Mechanics and Mining Sciences, 2015, 80: 337−345.

[33] WEN Tao, TANG Hui-ming, MA Jun-wei, et al. Deformation simulation for rock in consideration of initial damage and residual strength[J]. Earth Science, 2019, 44(2): 652−663.